Royal Netherlands
Meteorological Institute
Ministry of Infrastructure and the Environment

On the sea-surface drag and heat/mass transfer at strong winds

V. Kudryavtsev, V. Makin, S. Zilitinkevich

De Bilt, 2012 | Scientific report; WR 2012-02

On the sea-surface drag and heat/mass transfer at strong winds

Version 1.0

Date April 2012
Status Final

On the sea-surface drag and heat/mass transfer at strong winds

V. Kudryavtsev[1,2], V. Makin[3], S. Zilitinkevich[5,6,7,8]

[1]Russian State Hydrometeorological University, Russia

[2] NIERSC, St. Petersburg, Russia

[3]KNMI, De Bilt The Netherlands

[5]Finnish Meteorological Institute, Helsinki, Finland

[6]Division of Atmospheric Sciences, University of Helsinki, Finland

[7]A.M. Obukhov Institute of Atmospheric Physics, Moscow, Russia

[8]Department of Radio Physics, N.I. Lobachevski State University of Nizhniy Novgorod, Russia

Abstract

A simplified model for the sea surface momentum and enthalpy transfer coefficients are suggested. The main impact of droplets on the boundary-layer dynamics arises from the effect of the 'spray force' on the momentum balance of the air–spray mixture. The efficiency of the impact of spray via the 'stratification effect' is significantly weaker. The 'spray force' effect originates from the action of the vortex force on the marine atmospheric boundary layer (ABL) dynamics; this force results from the interaction of the 'rain of spray' with the wind shear. This effect leads to the acceleration of the airflow and the suppression of turbulence in the atmospheric boundary layer above the spray generation layer. It is shown that the drag coefficient C_{D10} levels off at a wind speed of around 30 m/s and further decreases with increasing the wind speed as approximately $\propto U_{10}^{-2}$. Action of the spray force results also in increase of the turbulent mixing coefficient in the spray generation layer. As a consequence, the vertical gradients of the "scalar" quantities (air temperature and humidity) in this layer are reduced with respect to the reference (no spray effect) gradients and are increased in the entire ABL above this layer. This in turn leads to the enhancement of the bulk transfer coefficient both for the sensible and latent heat. Both, suppression of the drag coefficient, C_{D10}, and increase of the enthalpy transfer coefficient, C_{E10}, result in rapid rise of the C_{E10}/C_{D10} ratio above the critical value of $C_{E10}/C_{D10} = 0.75$ at $U_{10} > 40$ m/s. Thus suggested model predicts that energy gain from enthalpy exceeds that lost from drag, providing the necessary conditions for tropical storms development.

1. Introduction

The vertical fluxes of momentum, sensible heat and latent heat (or water vapour) at the sea surface control the air-sea interaction processes at a range of scales from local to global and play a key role in numerous research areas and applications providing the boundary conditions for atmospheric and ocean models. Their realistic parameterization to a large extent determines the quality of weather and climate modelling. In operational models, the surface fluxes are parameterized in terms of the exchange coefficients for momentum, C_D, sensible heat, C_H and water vapour, C_E, also called the drag- and heat/mass-transfer coefficients (or, alternatively, in terms of the corresponding roughness lengths, z_0, z_T and z_E, directly linked to the exchange coefficients through the logarithmic wall law). For the low to moderate wind speeds, a general consensus has been achieved on the dependence of the above coefficients (or roughness lengths) on the mean wind speed, *U*, and fetch. In particular, it is recognised that z_0 (and therefore C_D) monotonically increases with increasing *U*, whereas the ratios $z_E / z_0 \sim z_T / z_0$ decrease, so that C_H and C_E only weakly depend on *U* (e.g., Zilitinkevich et al., 2001). However, at strong and extreme winds, the physical nature of the momentum- and heat/mass-transfer is still not fully understood, and even the general wind-speed dependence of the exchange coefficients remains rather uncertain.

There is indirect evidence that at strong winds C_D no longer increases with increasing *U* but, first, levels off and, at extreme winds, decreases. Emanuel (1995) and more recently Zweers et al. (2010) disclosed through numerical-modelling studies that tropical cyclones simulated using conventional parameterization of C_D (implying its continuous increase with increasing *U*) do not attain observed intensities and, moreover, to achieve the observed winds, C_D should be taken about three times smaller than it follows for the conventional parameterization. The first experimental evidence of the suppression of surface drag in hurricanes was reported by Powell et al. (2003, 2006) and later confirmed by Jarosz et al. (2007). They have found that C_D levels off and then, at wind speeds exceeding 34 m/s, decreases. French et al. (2007) carried out direct measurements of the momentum flux at strong winds and also detected levelling off the drag coefficient at wind speeds from 20 to 30 m/s.

Inspired by the above findings, Makin (2005), Barenblatt et al. (2005), Kudryavtsev (2006) and Rastigejev et al. (2011) developed theoretical models treating the sea-surface drag reduction analogously to the drag reduction in dust storms, as direct consequence of suppression of the surface-layer turbulence due to presumably strongly-stable stratification caused by suspended heavy particles (following Kolmogorov, 1954; Barenblatt, 1953; Beranblatt and Golitsyn, 1974). In all these studies, once the sea-surface drag model had been properly tuned, the required drag reduction was obtained but, admittedly, via artificial overestimation of the sea-spray concentrations. In particular, numerical experiments by Rastigejev et al. (2011) based on the Andreas (1998) spray generation function do not reveal any remarkable impact of the sea spray on the surface drag (see their Fig.3a); whereas similar calculations (see their Fig.3d) based on the strongly enhanced spray generation function [after Wu (1993), resulted at $U \sim 35$ m/s in the surface volume concentration of droplets of order 10^{-2} or the mass concentration of order 10, which is four orders of magnitude larger than it follows from the Andreas's function] demonstrates the strong impact. However, when mass concentration of spray well exceed 1, and thus density of the air-droplets mixture significantly deviates from the air one, the momentum conservation equation (normally used in Boissinesq approximation) losses its validity, and direct impact of spray on the momentum must be taken into account.

As distinct from the above theoretical models, Andreas (2004) considered the effect of the sea spray on the density stratification as insignificant. Instead he pointed to the impact of spray on the momentum balance consideration that a droplet, to be accelerated, extracts momentum from the air flow, so that the turbulent stress should be reduced in the spray generation layer but enhanced above this layer. Kudryavtsev and Makin (2011; hereinafter KM11) followed this idea and developed a theoretical model of the impact of spray on the momentum balance implying that the droplets affect the air flow basically through the "spray force" caused by the interaction of the "rain of spray" with the velocity shear. Such spray force just results in the acceleration of the air flow in the spray generation layer, and suppression of the turbulent stress above this layer. KM11 also demonstrated that at typically observed concentrations the stratification effect of spray is negligible compared to the spray-force effect.

In the present paper we employ the KM11 model to develop a practically oriented parameterization of the sea-surface drag and heat/mass transfer at strong and extreme winds typical of tropical cyclones (hurricanes and typhoons) and polar lows

2. Basic effects of the sea spray on drag reduction

a. Governing equations

At very high wind speeds, the sea droplets are torn off from the breaking waves and injected into the airflow at the height of the breaking-wave crests. This essential feature of the spray generation is taken into account in the mass- and momentum-conservation equations in the form of the volume source, V_s, defined as the rate of injection of droplets per unit volume (Fairall et al. 1990, 2009; Kudryavtsev 2006). A similar term, namely, the volume source of the momentum (the rate of injection of the momentum of droplets per unit volume) has never been taken into account and, to the best of our knowledge, it was first introduced in the moment conservation equation by KM11. With due regards to these volume sources, the conservation equations for the volume concentration of droplets, s, and the momentum become:

$$\frac{\partial}{\partial z}\left(\overline{s'w'}-\int a\hat{s}dr\right)=V_s\,, \tag{1}$$

$$\frac{\partial}{\partial z}\left(\rho\overline{u'w'}\right)=\rho_w F_s\frac{\partial U}{\partial z}\,, \tag{2}$$

where $\overline{s'w'}$ and $\rho\overline{u'w'}$ are vertical turbulent fluxes of the droplet concentration and momentum, respectively; a is the terminal fall velocity depending on the droplet radius r; $\hat{s}(r)$ is the droplet concentration spectrum [so that s is the integral of $\hat{s}(r)$ over radii]; ρ_w is the water density; $\rho=\rho_a(1+\sigma s)$ is the air-droplet mixture density, where $\sigma=(\rho_w-\rho_a)/\rho_a$ and ρ_a is the air density; and F_s is the volume flux of droplets, commonly known as the spray generation function (SGF) defined via the volume source V_s as

$$F_s=\int_z^\infty V_s dz\,. \tag{3}$$

The right-hand side of Eq. (2) represents the "vortex force" acting on the airflow due to interaction of rain of spray with the velocity shear. This force has a clear physical meaning: because permanent injection of droplets is compensated by their gravitational fall (so that $F_s=\int a\hat{s}(r)dr$), the droplets moving downward through the velocity shear are affected by the vortex force, and since these droplets are embedded in the airflow, they push the air particles stimulating acceleration of the airflow.

It is worthy to notice the following: KM11 deriving eq. (2) suggested that the droplets are "launched" on an altitude above the breaking crest with velocity equal to the wind velocity on that altitude, i.e. they are accelerated instantaneously once generated. The question may arise:

how does the model (2) take into account the force acceleration of droplets to the wind velocity? In order to clarify this point, let us rewrite eq. (2) in the form

$$\tau(z) = \rho_w \left[\int_z^\infty V_s U dz - F_s U(z) \right] + \rho_a u_*^2 ,$$

where $\tau(z) \equiv -\rho \overline{u'w'}$ is the local turbulent stress, and u_* is the friction velocity well above the surface. To derive this equation we have integrated (2) from "infinity" (where concentration of droplets is negligibly small) to a level z. This equation describes momentum exchange between droplets and air particles. Term in the square brackets in the r.h.s of this equation can be called as "the spray stress", τ_{sp}

$$\tau_{sp} = \rho_w \left[F_s U(z) - \rho_w \int_z^\infty V_s U dz \right].$$

The first term in τ_{sp} describes impact of droplets on the air momentum (due to the redistribution of the momentum between droplets and air particles), and the second term –effect of injection of the droplets momentum. At the sea surface $U(0) = 0$, therefore the turbulent stress, $\tau(+0)$, at the lower part of the atmospheric boundary layer but just above the water surface, reads

$$\tau(+0) = \rho_w \int_0^\infty V_s U dz + \rho_a u_*^2$$

This equation shows that the force applied to the lower part of the atmospheric boundary is a sum of the stress $\rho_a u_*^2$ associated with the form drag of the sea surface (that can be parameterized e.g. in terms of the Charnock roughness scale) and additional force required to accelerate detached droplets to the wind velocity on altitude of their injection. This force acts just above the breaking wave crests, however considering the atmospheric boundary layer over "rectifiable" surface; this force is finally emerged as force acting at the mean surface $z = z_0$.

b. Closure

KM11 employed the traditional closure scheme for the turbulent fluxes of momentum and droplets: $\tau \equiv -\rho \overline{u'w'} = \rho K_M \partial U / \partial z$ and $q \equiv \overline{s'w'} = -K_S \partial s / \partial z$, took the eddy viscosity, K_M, equal to the eddy diffusivity, K_S, and expressed them after the Monin–Obukhov similarity theory:

$$K_M = K_S = K = \kappa (\tau / \rho)^{1/2} (z + z_0) / \Phi \qquad (4)$$

where κ = 0.4 is the von Karman constant, $\Phi \geq 1$ is a universal function of z/L_s determined from observations in the thermally stratified atmospheric surface layer, and L_s is the Obukhov length based on the buoyancy flux q:

$$L_s = (\tau/\rho)^{3/2} / \kappa g q . \tag{5}$$

The natural boundary conditions for U and s are

- at the surface ($z = 0$): $U = 0$ and $\partial s/\partial z = 0$ (vanishing turbulent flux of droplets);
- at a reference level well above the spray generation layer ($z = h$): $U = U_h$ and $s = 0$.

Integrating equations (1) and (2) under these conditions yields

$$\hat{s}(z,r) = \hat{s}_*(z,r) + \int_0^z \exp\left[-\int_{z'}^z \omega\Phi d\varsigma\right] a^{-1}\hat{V}_s dz' , \tag{6}$$

$$U(z) = \frac{u_*}{\kappa}\int_0^z \Phi d\varsigma + \int_0^z (u_s^h - u_s)\Phi d\varsigma . \tag{7}$$

Here, s and V_s marked with hats over denotes their spectra over the droplet radii (r); $\varsigma = \ln(z + z_0)$ is the integration variable; z_0 is the sea-surface roughness length specified by the Charnock relation:

$$z_0 = c_h^0 u_*^2 / g \tag{8}$$

with $c_h^0 = 1.4\times10^{-2}$ [as determined by Kudryavtsev and Makin (2007) for strong winds]; $\omega = a/\left(\kappa\sqrt{\tau/\rho}\right)$ is the dimensionless fall velocity; $s_* = \hat{F}_s / a$ is the equilibrium droplet concentration corresponding to the balance between the rates of injection and gravitational subsidence; u_s is the "spray-forced wind velocity":

$$u_s(z) = (2\kappa^2)^{-1}\sigma\int_0^z F_s\Phi d\varsigma ; \tag{9}$$

$u_s^h = u_s(h)$ is the spray-forced velocity at $z = h$ (i.e. well above the spray-generation layer); and u_* is the friction velocity at $z = h$ determined by the resistance law:

$$C_{dh} = (u_*/U_h)^2 = \kappa^2\left[\int_0^h \Phi d\varsigma + (\kappa/u_*)\int_0^h (u_s^h - u_s)\Phi d\varsigma\right]^{-2} , \tag{10}$$

where C_{dh} is the drag coefficient.

As follows from the above equations, the sea droplets generally affect the dynamics of the marine atmospheric boundary layer (MABL) in two ways:

- through suppression of turbulent mixing by the density stratification [described by the stratification function $\Phi(z/L_s)$],
- through the action of the spray force on the momentum of the spray-air mixture (described by the spray-forced velocity u_s).

As seen from equations (7) and (10), each of these mechanisms could lead to the acceleration of airflow and reduction of the sea surface drag. KM11 considered both of them and demonstrated that in natural conditions the first one (stratification) is practically inefficient, and the observed drag reduction is quite naturally explained by the spray force action. Below we neglect the effect of stratification and thus essentially simply the KM11 model.

The key element of the problem in question is the spray-generation function, which determines the vertical profiles of the spray concentration and the wind velocity, equations (6) and (7), and the drag coefficient, equation (10). Although the spray-generation function (SGF) is currently known with great uncertainty (Andreas, 2002), for our purposes it is sufficient to know that, in terms of the volume flux the empirical SGF has the quadratic spectral shape, $\widehat{F}_s(r) \propto r^2$, with the spectral cut-off at the droplet radii ranged from $r_0 \approx 200\mu m$ [after Andreas (2002) field data] to r_0 of order 1mm [after Anguelova et al. (1999) and Fairall et al. (2009) laboratory data]. In both cases the spume droplets related to the maximum in the SGF spectrum ($r \sim r_0$) can be treated as heavy droplets with the dimensionless terminal fall velocity $\omega >> 1$. Then, because the integral SGF, $F_s = \int \widehat{F}_s(r)dr$, is basically determined by the largest droplets, the large-ω approximation is sufficient for our analysis.

c. Simplification

For the sake of simplicity, we approximate the vertical distribution of the SGF by the step-like function

$$F_s(u_*, z) = F_s^0(u_*)H(1 - z/d)\,, \qquad (11)$$

where $F_s^0(u_*)$ is the spray flux at the surface, $H(x)$ is the Heaviside function [$H(x) = 1$ at $x > 0$, and $H(x) = 0$ at $x < 0$], d is the depth of the spray generation layer, linked to the wave number k_b of shortest breaking wave producing spume droplets: $d = 2k_b^{-1}$. Then the vertical profile of the volume source, V_s, becomes the delta-function; and at $\omega >> 1$, with the accuracy to $1/\omega$, Eq. (6) simplifies to

$$\hat{s}(z,r) \approx \hat{s}_*(z,r)(z'/d)^{-\omega}, \tag{12}$$

where $z' = \max(d,z)$. This relation states that inside the spray generation layer the droplet concentration is controlled by the balance between the breaking crests tearing and gravitational settling; and this layer it sharply decreases due to inefficiency of the turbulent transport of heavy droplets.

As follows from Eq. (1), in this approximation the turbulent flux of droplets turns into zero at $z < d$, and becomes $q \approx F_s^0 (z/d)^{-\omega_0}$ at $z \geq d$, where $\omega_0 = \omega(r_0) >> 1$. Correspondingly, the Obukhov length Eq. (5) has a finite value in a thin layer around $z = d$, with thickness of order d/ω_0. The effect of stratification on the momentum balance is characterized by the integral $I = \int_0^h L_s^{-1} dz \approx \kappa g d \omega_0^{-1} F_s^0 / (\tau/\rho)^{3/2}$ and becomes negligible when $I << 1$. KM11 solved the problem numerically and, for reasonably determined SGF and $\omega_0 >> 1$, estimated that the integral I is small as compared to unity up to the highest possible wind speeds. Hereinafter, we neglect the stratification mechanism by setting $\Phi = 1$.

Then specifying the SGF by Eq. (12), the velocity profile (7) and resistance law (10) become

$$\frac{\kappa U(z)}{u_*} = \ln\left[(z+z_0)/z_0\right] + \frac{\sigma F_s^0}{4\kappa u_*}\left[\ln^2(d/z_0) - \ln^2(d/z')\right], \tag{13}$$

where $z' = \min(z+z_0, d)$, and

$$C_{Dh} \equiv \left(u_*/U_h\right)^2 = \kappa^2 \left[\ln(h/z_0) + \frac{\sigma F_s^0}{4\kappa u_*}\ln^2(d/z_0)\right]^{-2}. \tag{14}$$

Both empirical data (Andreas, 1999) and prior theoretical analysis (Kudryavtsev and Makin, 2009) demonstrate that the SGF sharply increases with the increasing wind speed: $F_s^0 \propto u_*^4$, so that equations (13) and (14) describe the acceleration of airflow and the drag reduction with the increasing wind speed. The term describing the impact of spume droplets on C_{Dh} increases very rapidly – as u_*^3. However, its significance thoroughly depends on the surface value of the SGF.

Following KM11, we identify the depth of the spray generation layer, d, with the inverse wave number of the shortest breaking waves producing spume droplets. Alternatively, d is linked to the significant-wave height (e.g., Andreas, 2004). Because d appears in Eq. (14) under the logarithm, the drag coefficient, C_{Dh}, is rather insensitive to its choice.

3. Parameterization

a. Spray generation function

As already motioned, the spray generation model proposed by Kudryavtsev and Makin (2009) and modified by KM11 is based on the assumption that the droplets torn off from the crests of breaking waves are injected into airflow at the level of breaking waves. Pulverization of the water/foam into droplets takes place in a thin boundary layer adjacent to each breaking wave crest. The rate of the droplet production from individual breaking crests is proportional to the wind speed; the size distribution of the droplet volume concentration is proportional to r^2; and the total volume production of droplets is proportional to the total length of the wave breaking fronts, where the main contribution comes from the shortest breaking waves with the wave number $k = k_b$. At moderate wind speeds (less than 15 m/s), the wave number of the shortest breaking waves carrying white caps is $k_b \approx 5$ rad/m (Gemmrich et al., 2008). At higher wind speeds, crests of the shorter breaking waves, not visible as white caps, are disrupted by the wind due to the Kelvin–Helmholtz instability. Then the upper limit of breaking waves producing droplets extends towards smaller scales, up to $k_b \approx 25$ rad/m. This expansion of the range of breaking waves capable of atomising into droplets, results in the “explosive” growth of the SGF.

KM11 have chosen the SGF model parameters by fitting to the empirical function of Andreas (1998) and laboratory data on the spray generation of Fairall et al. (2009), Koga (1981) and Anguelova et al. (1999) shown in Figure 1. This model is simplified without loss of accuracy taking

$$F_s^0 = c_s u_*(u_{10} / c_b)^3 , \tag{15}$$

where $c_s = 1.6\times10^{-9}$ is an empirical constant, and $c_b = c(k_b)$ is the phase velocity of the shortest breaking waves producing spume droplets. Its wave number k_b is defined as

$$k_b = \max(k_{wc}, k_{wb}) , \tag{16}$$

where $k_{wc} = 5$ rad/m is the wave number of the shortest breaking waves generating white caps, and k_{wb} is the upper limit of the range of wind waves whose breaking crests are disrupted aerodynamically by the Kelvin-Helmholtz instability. KM11 determined k_{wb} as

$$k_{wb} = \sqrt{g/\gamma}\min\left[5.5\times10^{-2}(0.04u_{10}/u_*^{cr} - 1.2), 0.07\right], \qquad (17)$$

where γ is the water surface tension, and $u_*^{cr} = 0.45$ m/s is the critical friction velocity. Equations (15)-(17) comprise the proposed very simple parameterization.

Figure 1 shows the SGF versus the wind speed at 10-m height, u_{10}, after KM11 (solid line), our parameterization (dotted line) and empirical data. Sharp growth of the spume droplet production at wind speeds from 15 to 20 m/s results from the Kelvin–Helmholtz instability leading to the disruption of the crests of short breaking waves. The dashed line show the so-called “heuristic” SGF deduce by Andreas (1998) from his empirical SGF multiplied by the factor of 10 – to fit it to modelling the effect of spray on the intensity of tropical cyclones (Andreas and Emanuel, 2001). Open circles and triangles show the Fairall et al. (2009) and Toffoli et al. (2011) laboratory data. We emphasise that the spume-droplet flux sharply decreases above the breaking wave crests. Because the laboratory measurements were carried out in the layer between 15 and 30 cm above the crests, it is natural that the laboratory values of SGF are much smaller than the surface values. Within the order of magnitude, the KM11 model and our approximation, equations. (15)-(17), are consistent with empirical data. It is worth noticing that the shape of the wind-speed dependence of SGF according to the KM11 model or Eq. (15) almost perfectly coincides with its shape in laboratory experiments.

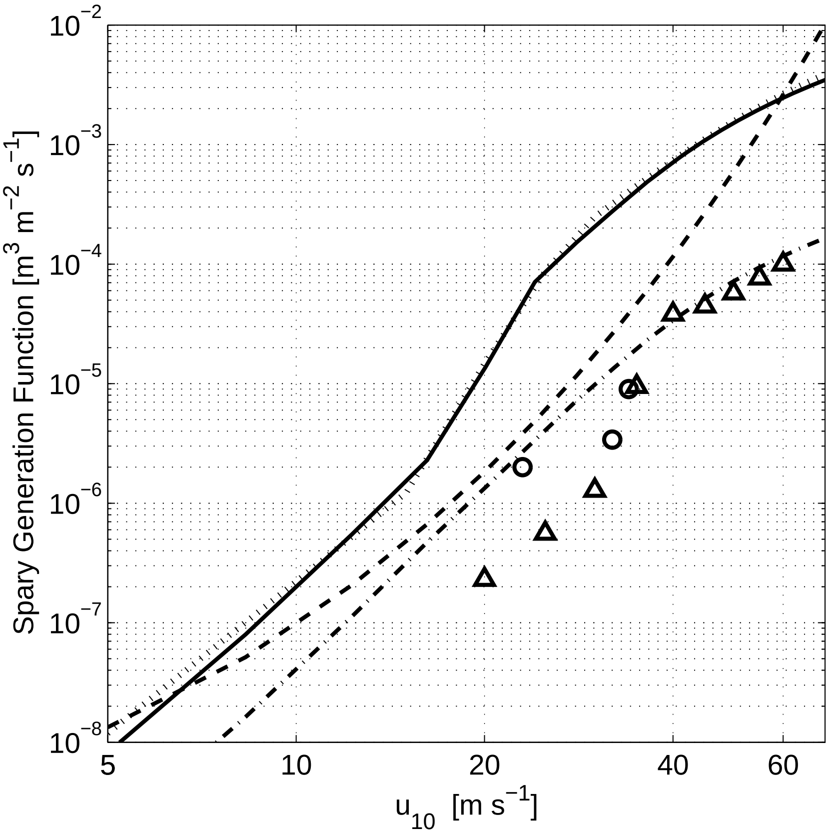

Figure 1. The spume-droplet spry generation function (SGF) versus the wind speed at 10 m height, u_{10}. The dashed line shows the Andreas (1998) "heuristic" SGF; the solid and dashed-dotted lines, the SGF at the surface and at 30 cm height, respectively, after the KM11 model; and the dotted line, our parameterization, Eq. (15). Open circles show the Fairall et al. (2009) laboratory measurements in the layer from 15 to 30 cm; and open triangles, the Toffoli et al. (2011) laboratory measurements (their Fig.4).

b. *Drag coefficient*

Substituting Eq. (15) for $F_s^{(0)}$ in Eq. (14), the drag coefficient is expressed as:

$$C_{Dh} \equiv \left(u_* / U_h\right)^2 = \kappa^2 \left[\ln(h / z_0) + \Delta_m\right]^{-2}, \tag{18}$$

where z_0 is the Charnock's aerodynamic roughness length, Eq. (8), and the term Δ_m describes the impact of the spume droplets:

$$\Delta_m = c_m (u_{10} / c_b)^3. \tag{19}$$

Here, the dimensionless coefficient $c_m = c_s \sigma / (4\kappa) \ln^2(d / z_0) = 6.4 \times 10^{-6}$ can be taken as constant. Indeed, with the increasing wind speed, the friction velocity at the sea surface, u_*, has a tendency to level off (due to the drag reduction), which is why the combination $\ln^2(d/z_0)$, generally dependent on u_*, also levels off.

In the last decade serious efforts we made to investigate experimentally the wind-speed dependences of the drag coefficient, $C_{D10} = (u_*/u_{10})^2$, and friction velocity, u_*. Powell et al. (2003) analyzed 331 profiles obtained by GPS sondes, dropped in 15 storms from 1997 to 1999 and revealed levelling off of the surface stress at wind speed exceeding 34 m/s. Powell (2006) extends this analysis to 2664 GPS-sonde profiles covering the period 1997-2005 and including wind speeds up to 80 m/s. The extended dataset evidenced that the drag coefficient generally decreases from its maximal value, exceeding $2 \cdot 10^{-3}$, to less than 10^{-3} at wind speeds > 50 m/s, which corresponds to levelling of the friction velocity at u_* between 1.5 and 2 m/s. As seen from Figure 2, these essential features of the sea-surface drag at strong winds are quite well reproduced by the proposed parameterization. At u_{10}< 20 m/s it coincides with the Charnock relation, Eq. (8), implying unlimited grows of both C_{D10} and u_*, but at stronger winds it fully deviates from Eq. (8) and almost perfectly reproduces observed decrease in C_{D10} associated with levelling off u_*. Independent data of Jarisz et al. (2007) also shown in Figure 2 basically confirm the above conclusions.

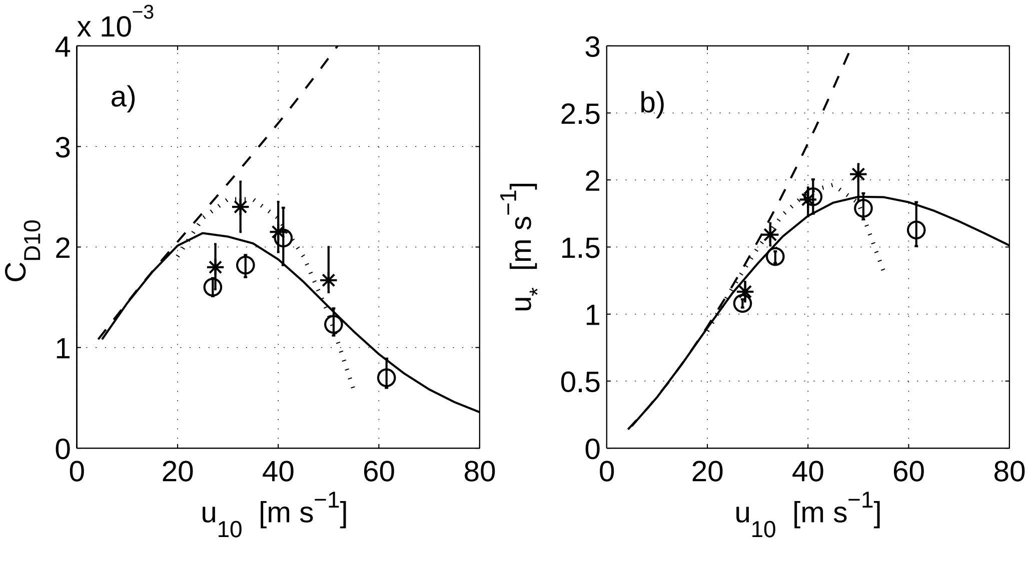

Figure 2. The wind-speed dependences of the drag coefficient C_{D10} for h = 10 m (a) and the friction velocity u_* (b). Solid lines are plotted after Eq. (18) accounting for the effect of spray; dashed lines, after the Charnock relation, Eq. (8), disregarding this effects. Open circles show experimental data from Fig. 7 of Powell (2006), stars show similar data from Fig.3 of Powell et al. (2003). Vertical lines indicate the 95% confidence limits. Both data sets are obtained from

measurements between 20 and 150 m above the surface. Dotted lines show the quadratic polynomial approximation of data from Figure 3 of Jarosz et al. (2007).

The resistance law, equations (18)-(19), can be expressed through the effective roughness length, Z_0:

$$C_{Dh} = \kappa^2 / \ln^2(h / Z_0) \tag{20}$$

where

$$Z_0 = c_h^0 \frac{u_*^2}{g} \exp(-\Delta_m) \,. \tag{21}$$

Alternatively, the resistance law can be presented in terms of the wind-speed dependence of the "Charnock parameter", defined as $Z_0 g / u_*^2$ and tuning into the Charnock constant, c_h^0, at $u_{10} < 20$ m/s. In Figure 3 we use this format to illustrate dramatic inconsistency of the traditional sea-surface drag formulation at wind speed exceeding 30 m/s.

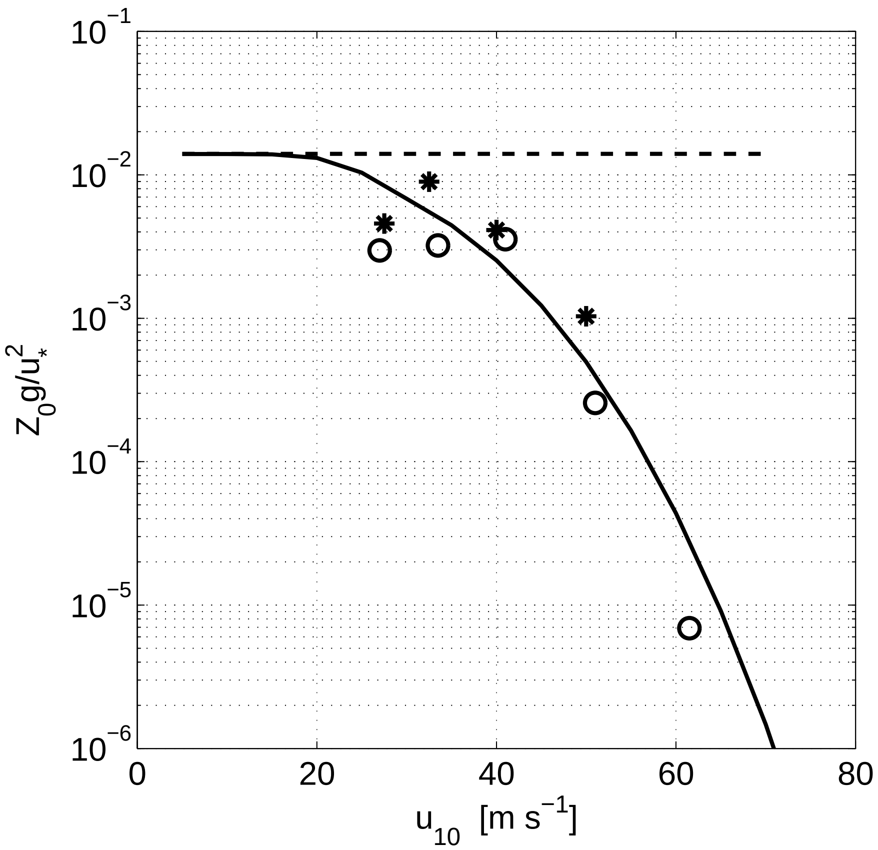

Figure 3. The wind-speed dependence of the Charnock parameter, $c_h = Z_0 g / u_*^2$. The dashed line shows its reference (no-spray) value. The solid line is plotted after Eqs. (19) and (21). Circles and starts show the same data of Powel et al. (2003, 2006) as in Figure 2.

As shown by KM11 (see their Fig.1c), in the presence of droplets the turbulent stress in MABL is no longer constant with height. Using Eq. (13), the "local friction velocity", $\sqrt{\tau/\rho} = \kappa(z+z_0)\partial U/\partial z$, is expressed as

$$\sqrt{\tau/\rho} = u_*\left[1+\frac{\sigma}{2\kappa}\frac{F_s^0}{u_*}\ln\left(\frac{d}{z'}\right)\right], \qquad (22)$$

where $z' = \min(z+z_0, d)$. Above the spray generation layer, it turns into u_*, and inside the layer, at $z < d$, it grows toward the surface From (22) using (15), the turbulent shear stress $\tau_s = \tau(0)$ acting on the lower part of the atmospheric boundary layer can be parameterized as

$$\tau_s/\rho = u_*^2\left(1+\Delta_\tau\right)^2 \qquad (23)$$

where $\Delta_\tau = c_\tau(u_{10}/c_b)^3$ with $c_\tau = c_s\sigma/(2\kappa)\ln(d/z_0) = 4.5\times10^{-6}$, where following the above reasoning the "slowly" varying function $\ln(d/z_0)$ is absorbed in the constant. Near-surface stress (23) is larger than the turbulent stress in the core of MABL (above spray generation layer). We remind, that within the frame of the considered model, there is the stress discontinuity at the surface: the difference between τ_s and stress acting on the water surface $\rho_a u_*^2$ (from drag) is the force required to accelerated the droplets to the wind velocity.

c. *Enthalpy transfer coefficient*

The question now, - is such a model behaviour of the drag coefficient sufficient for improvement of the tropical storms and polar lows modeling and forecast. Emanuel (1986, 1995) found that the maximum predicted wind speed is proportional to the ratio of the bulk coefficients for enthalpy (C_{K10}) and momentum, C_{K10}/C_{D10} and the most plausible range of C_{K10}/C_{D10} is 1.2 to 1.5, with a lowest value of 0.75. For $C_{K10}/C_{D10} < 0.75$ the energy lost due to drag exceeds that gained from enthalpy, and tropical storms die down. However the ratio of existing standard enthalpy and momentum coefficient, calculated according the traditional parameterizations is about 0.5 and decreases if these coefficients are extrapolated to high winds (see e.g. Fig.6 below). Thus if these values of the coefficients are used, the hurricane will not develop. As noted by Drennan et al. (2007), the present operational hurricane model uses a bulk flux algorithm where the roughness lengths for humidity and temperature are equal to the aerodynamic roughness length. This fact clearly does not support the data, but meets the Emanuel criterion, that presumably explains why such an algorithm is used in hurricane models.

Enthalpy is the sum of the sensible heat and latent heat, and its turbulent flux is the sum of corresponding heat fluxes. We assume that surface roughness length for temperature (z_{0t}) and humidity (z_{0q}) are the same, $z_{0t} = z_{0q}$ (see e.g. Zhang et al., 2008). In the present study we ignore the impact of droplets evaporation on sensible and latent heat balance. In this case the enthalpy transfer coefficient, C_{K10}, is equal to either sensible, C_{H10}, or latent, C_{E10}, heat transfer coefficient. We consider below behaviour of the latent heat transfer coefficient keeping in mind that obtained relation describes as well the enthalpy transfer coefficient.

Ignoring the impact of droplets evaporation, the humidity balance reads:

$$E = K\partial q / \partial z = const, \tag{24}$$

where q is the specific humidity, E is its turbulent flux, and $K = \kappa z\sqrt{\tau / \rho}$ is the turbulent eddy viscosity coefficient where local friction velocity is defined by (22). Then the gradient of the humidity reads

$$\frac{\partial q}{\partial z} = \frac{E}{\kappa u_* z}\left[1 + \frac{\sigma}{2\kappa}\frac{F_{s0}}{u_*}\ln\left(\frac{d}{z'}\right)\right]^{-1} \tag{25}$$

where $z' = \min(z + z_0, d)$, and shows that due to enhanced turbulent mixing, vertical gradient of the humidity in the spray generation layer, z<d, is increased relative to its value in the layer above. Equation (25) can be integrated from the low bound $z = z_{0q}$ (z_{0q} is the roughness scale for humidity) to arbitrary height z. For the heights above spray generation layer>d, the vertical distribution of humidity reads:

$$\begin{aligned} q(z) - q_s &= \frac{E}{\kappa u_*}\left\{\ln\left(z / z_{0q}\right) - \ln\left(d / z_{0q}\right)\left[1 - \Delta_\tau^{-1}\ln\left(1 + \Delta_\tau\right)\right]\right\} \\ &= \frac{E}{\kappa u_*}\ln(z / Z_{0q}) \end{aligned} \tag{26}$$

where q_s is specific humidity at the surface, parameter Δ_τ is the same as in (23), and Z_{0q} is the effective roughness scale for humidity accounting for the impact of spray:

$$Z_{0q} = z_{0q}(d / z_{0q})^{1-\ln(1+\Delta_\tau)/\Delta_\tau} \tag{27}$$

Calculations of the effective roughness length Z_{0q} are shown in Fig.4. At small Δ_τ the effective roughness scale Z_{0q} equals the local roughness scale z_{0q} and the humidity profile (26) is reduced to the “standard” log-profile $\propto \ln(z / z_{0q})$. At high wind speeds, when parameter Δ_τ is expected to be large, the effective roughness scale is growing towards the depth of the spray generation layer: $Z_{0q} \to d$.

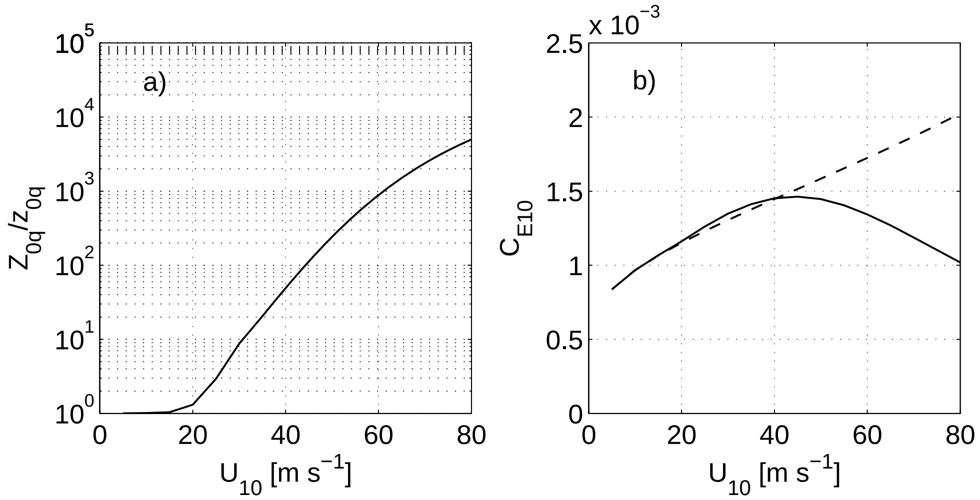

Figure 4. a) The effective humidity roughness length Z_{0q} defined by (25) scaled by the reference value z_{0q} vs wind speed. Thick dash line indicates its model asymptotic value corresponding to the spray generation layer depth. **b)** Humidity transfer coefficient defined by (28) or (27) (solid line) and the reference one (dash line) vs. wind speed.

Equation (26) gives the following relation for the humidity bulk transfer coefficient $C_{E10} = E / \left[(q_{10} - q_s) u_{10} \right]$:

$$C_{E10} = \frac{\kappa}{\left\{ \ln(10 / z_{0q}) - \ln(d / z_{0q}) \left[1 - \Delta_\tau^{-1} \ln\left(1 + \Delta_\tau\right) \right] \right\}} C_{D10}^{1/2}, \qquad (28)$$

that can be also expressed in terms of the effective roughness scale for the momentum, Eq.(21), and humidity, Eq.(25), as

$$C_{E10} = \frac{\kappa^2}{\ln(10 / Z_{0q}) \ln(10 / Z_0)}. \qquad (27)$$

Calculations of the reference (impact of spray is ignored) and the model humidity bulk transfer coefficient defined by Eq. (28) or (27) are shown in Fig.4b. In these calculations the reference humidity roughness scale is specified as $z_{0q} = 10^{-6}$. The reference calculations are performed on (28) at $\Delta_\tau = 0$. The behaviour of C_{E10} with increasing winds results from an interplay between fast growth of the effective roughness length for humidity Z_{0q} (see Fig.4a) and rapid fall of the effective roughness length for momentum Z_0 (see Fig.3). At wind speed above 20 m/s enhanced turbulent mixing in the spray generation layer, and growth of Z_{0q} compensates levelling off of C_{D10}, therefore C_{E10} continues to grow. However, at wind speeds $U_{10} > 40$ m/s suppression of the roughness length prevails over the Z_{0q} growth, and thus C_{E10} is levelling off and then decreases at higher winds.

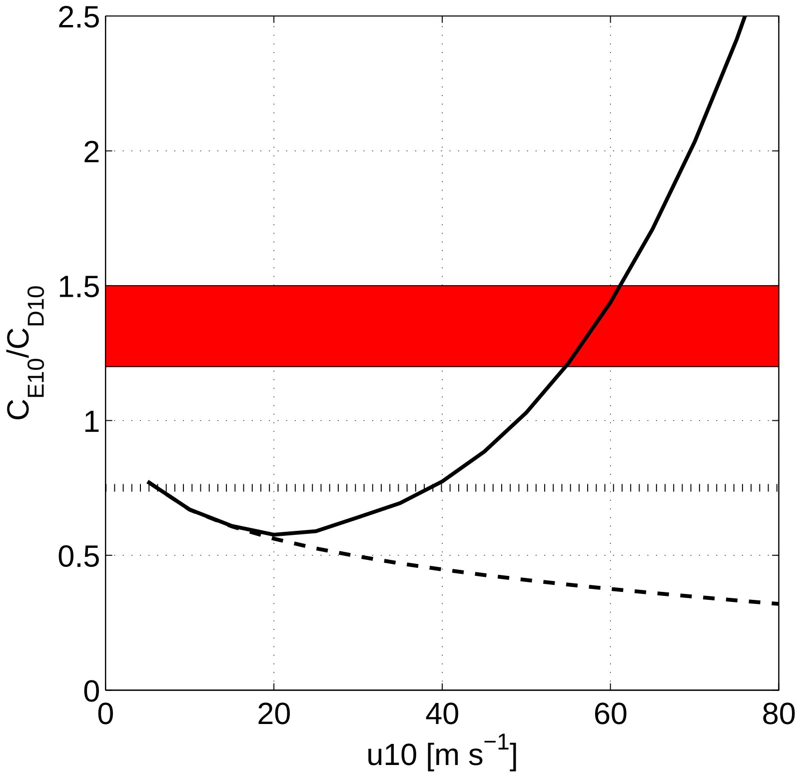

Figure 5. Ratio of the humidity and the momentum transfer coefficients. Dash line is reference run (no spray effect), solid line is ratio of model C_{E10} defined by (28) (or (27)) to the model C_{D10} defined by (20). Dotted line indicates the critical level $C_{E10} / C_{D10} = 0.75$ introduced by Emanuel (1995). For $C_{E10} / C_{D10} < 0.75$ the energy lost to drag exceeds that gained from enthalpy, and tropical storms die down. Shaded area indicates the most plausible range of the ratio suggested by Emanuel (1995): $1.2 < C_{E10} / C_{D10} < 1.5$.

The ratio of the humidity to the momentum transfer coefficients is shown in Fig.5. The reference ratio (shown by dash line) is significantly lower than the critical value $C_{E10} / C_{D10} = 0.75$ for hurricane development (Emanuel, 1995). At wind speeds above 20 m/s the model ratio accounting for the impact of spray, deviates from the reference values and at wind speeds above 40 m/s exceeds the threshold value. In the range of wind speed range 55 m/s to 60m/s the model ratio corresponds to the most plausible value of C_{E10} / C_{D10} from 1.2 to 1.5

suggested by Emanuel (1995), and continues to grow at higher winds. In the wind speed range from 20 m/s to 30 m/s the model values are consistent with the mean value $C_{E10} / C_{D10} = 0.63$ reported by Drennan et al. (2007) and Zhang et al. (2008) after their direct measurements of momentum and enthalpy flux within the atmospheric boundary layer of a hurricane.

4. **Conclusion**.

Thus, the proposed simplified model/parameterizations are capable of predicting the suppression of the surface drag at high wind speeds as a consequence of a reasonable choice of the model parameters related to the spray generation. The main impact of droplets on the boundary-layer dynamics arises from the effect of the 'spray force' on the momentum balance of the air–spray mixture. The efficiency of the impact of spray via the 'stratification effect' is significantly weaker. The 'spray force' effect originates from the action of the vortex force on the MABL dynamics; this force results from the interaction of the 'rain of spray' with the wind shear. This effect leads to the acceleration of the airflow and the suppression of the turbulence in the ABL above the spray generation layer. It is shown that the drag coefficient C_{D10} levels off at a wind speed of around 30 m/s and further decreases with increasing the wind speed as approximately $\propto U_{10}^{-2}$. This trend in C_{D10} is in agreement with experimental data of Powell et al. (2003), Powell (2006) and Jarosz et al. (2007) acquired in hurricanes.

Action of the spray force results also in increase of the turbulent mixing coefficient in the spray generation layer. As a consequence, the vertical gradients of the "scalar" quantities (air temperature and humidity) in this layer are reduced with respect to the reference (no spray effect) gradients and are increased in the entire ABL above this layer. This in turn leads to the enhancement of the bulk transfer coefficient both for the sensible and latent heat. Both, suppression of the drag coefficient, C_{D10}, and increase of the enthalpy transfer coefficient, C_{E10}, result in rapid rise of the C_{E10} / C_{D10} ratio above the critical value of $C_{E10} / C_{D10} = 0.75$ at $U_{10} > 40$ m/s. Thus suggested model predicts that energy gain from enthalpy exceeds that lost from drag, providing the necessary conditions for tropical storms development. Suggested parameterizations can be tested and implemented in numerical atmospheric, storm surge and wind wave models, - especially in the range of high wind speed conditions, when standard parameterization of the drag and heat transfer coefficients are not valid.

Acknowledgements: This work has been supported by the ONR Grant N00014-08-1-0609, the EC FP7 ERC Grant No. 227915, and the Russian Federation Government Grants: No. 11.G34.31.0078 for the Russian Sate Hydrometeorological University, and No. 02.740.11.5225 for the N.I. Lobachevski State University of Nizhniy Novgorod. We also acknowledge the intensive and fruitful discussions with Gerrit Burgers and Niels Zweers

References:

Andreas EL (1998) A new spray generation function for wind speeds up to 32 m/s. J Phys Oceanogr 28:2175–2184

Andreas EL (2004) Spray stress revised. J Phys Oceanogr 34:1429–1440

Andreas EL, Emanuel KA (2001) Effect of sea spray on tropical cyclonic intensity. J Atmos Sci 58:3741–3751

Anguelova M, Barber RP, Wu J (1999) Spume drops produced by the wind tearing of wave crests. J Phys. Oceanogr 29:1156–1165

Barenblatt GI, Golitsyn GS (1974) Local structure of mature dust storms. J Atmos Sci 31:1917–1933

Barenblatt GI, Chorin AJ, ProstokishinVM (2005) A note concerning the Lighthill sandwich model of tropical cyclones. Proc Natl Acad Sci USA 102:11148–11150

Black PG, D'Asaro EA, Drennan WM, French JR, Niiler PP, Sanford TB, Terrill EJ, Walsh EJ, Zhang JA (2007) Air-sea exchange in hurricanes synthesis of observations from the coupled boundary layer air-sea transfer experiment. Bull Am Meteorol Soc 88:357–374

Bye JAT, Jenkins AD (2006) Drag coefficient reduction at very high wind speeds. J. Geophys Res 111:C033024. doi:10.1029/2005JC003114

Drennan WM, JA Zhang, J.F. French, C. McCormick, and PG Black (2007) Turbulent Fluxes in the Hurricane Boundary Layer. Part II: Latent Heat Flux. J. Atm. Sci., 64, DOI: 10.1175/JAS3889.1, 1103 - 1115

Emanuel KA (1995) Sensitivity of tropical cyclones to surface exchange coefficients and a revised steady-state model incorporating eye dynamics. J Atmos Sci 52:3969–3976

Fairall CW, Edson JB, Miller MA (1990) Heat fluxes, white caps, and sea spray. In: Geernaert GL, Plant WJ (eds) Surface waves and fluxes, vol 1. Kluwer, Dordrecht, pp 173–208

Fairall CW, Banner ML, Peirson WL, Asher W, Morison RP (2009) Investigation of the physical scaling of sea spray spume droplet production. J Geophys Res 114:C100001. doi:10.1029/2008JC04918

Gemmrich J, Banner M, Garrett C (2008) Spectrally resolved energy dissipation rate and momentum flux of breaking waves. J Phys Oceanogr 38. doi:10.1175/2007JPO3762.1

Jarosz E, Mitchell DA, Wang DW, Teague WJ (2007) Bottom-up determination of air-sea momentum exchange under a major tropical cyclone. Science 315:1707–1709

Koga M (1981) Direct production of droplets from breaking wind-waves—its observation by a multi-colored overlapping exposure photographing technique. Tellus 33:552–563

Kudryavtsev VN (2006) On effect of sea droplets on atmospheric boundary layer. J Geophys Res 111:C07020. doi:10.1029/2005JC002970

Kudryavtsev VN, Makin VK (2007) Aerodynamic roughness of the sea surface at high winds. Boundary-Layer Meteorol 125:289–303

Kudryavtsev VN, Makin VK (2009) Model of the spume sea spray generation. Geophys Res Lett 36:L06801. doi:10.1029/2008GL036871

Kudryavtsev V., and V. Makin (2011), Impact of ocean spray on the dynamics of the marine atmospheric boundary layer, Boundary Layer Meteorol., DOI 10.1007/s10546-011-9624-2

Makin, V.K.(2005) A note on drag of the sea surface at hurricane winds Boundary-Layer Meteorol., 115:169-176.

Powell MD (2006) Drag coefficient distribution and wind speed dependence in tropical cyclones. Final report to the National Oceanic and Atmospheric Administration, Joint Hurricane Test bed Program, Miami, 26 pp

Powell MD, Vickery PJ, Reinhold TA (2003) Reduced drag coefficient for high wind speeds in tropical cyclones. Nature 422:279–283

Jun A. Zhang,1,2 Peter G. Black,3,4 Jeffrey R. French,5 and William M. Drennan1, (2008), First direct measurements of enthalpy flux in the hurricane boundary layer: The CBLAST results. Geoph. Res. Letters, 35, L14813, doi:10.1029/2008GL034374, 2008

Zilitinkevich, S.S., Grachev, A.A., and Fairall, C.W., 2001: Scaling reasoning and field data on the sea-surface roughness lengths for scalars. *J. Atmos. Sci.*, **58**, 320-325.

Zweers, J.W. Makin, V.K, de Vries and G.J.H. Burgers, (2010) A sea drag relation for hurricane wind speeds, Geophys. Res. Lett., 37: L21811, doi:10.1029/2010GL045002, 2010.

A complete list of all KNMI-publications (1854 – present) can be found on our website

www.knmi.nl/knmi-library/knmipub_en.html

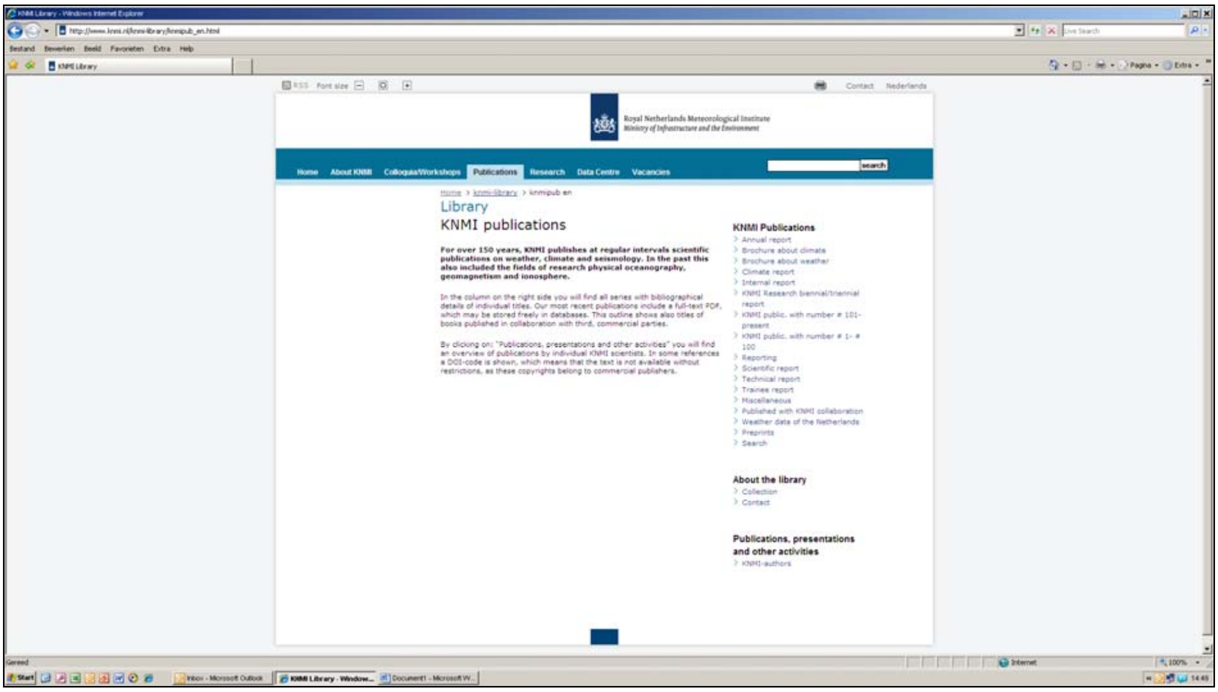

The most recent reports are available as a PDF on this site.